Influence of grease lubrication on freeting-fatigue damages of steel wire ropes

S. Montalvo, Siegfried Fouvry, Mickael Martinez

Proceedings of the ASME 2022 41st International Conference on Ocean, Offshore and Arctic Engineering
OMAE2022
June 5-10, 2022, Hamburg, Germany

OMAE2022-79102

INFLUENCE OF GREASE LUBRICATION ON FRETTING-FATIGUE DAMAGES OF STEEL WIRE ROPES

S. Montalvo [a,b] , S. Fouvry [a] , M. Martinez [b]

(a) LTDS, Ecole Centrale de Lyon, Ecully, France
(b) IFPEN, Lyon, France

ABSTRACT

Steel wire ropes can be used as mooring lines for Floating Offshore Wind Turbines. Swell induces tension and bending in the line. Investigating the effects of combined loads on rope lifetime is necessary. In these cases, fretting-fatigue damage is considered to be one of the main causes of failure. To prevent corrosion, grease is injected in the rope. The effect of grease on the fretting-fatigue damage of two wires in contact was investigated. A multi-scale approach was applied to calculate representative local loads in the mooring ropes. Global tension and bending were applied to a detailed model of the rope to calculate the local stress and contact forces in the steel wires. These are the fretting-fatigue loads applied in the laboratory tests. Two series of fretting-fatigue tests were conducted, each one with clean and greased wires. A two actuators hydraulic rig was used, allowing for complete decoupling of the fretting and fatigue loads. In the first series, the fatigue load was kept constant, and the fretting load was changed. In partial slip regime, for small fretting amplitudes, greased wires have longer lifetimes than non-greased wires. In a second series of fretting-fatigue tests, this most critical fretting condition was used and kept constant, and the fatigue load was changed. Results show that the fatigue limits of clean and greased wires are equal.

Keywords: fatigue, cable, floating offshore wind turbines, experiment, finite element method

1. INTRODUCTION

The floater of a Floating Offshore Wind Turbine is anchored to the seabed with mooring lines, which are often made of chains at both ends and steel wire rope in between. Swell induces tension in the mooring line, as well as bending close to the floater and the seabed. The bending is thus concentrated in the chains, while the rope experiences only tension. Chains are the weak point of the mooring line, with a higher risk of fatigue rupture. Solutions have been proposed to connect directly the rope to the platform, avoiding the use of chains, but it would expose the rope to bending loads, in addition to the tension. Investigating the effects of combined tension and bending on rope lifetime is thus necessary.

Cyclic tension and bending generate fatigue in the wires constituting the rope, leading to the initiation and propagation of fatigue cracks. Cyclic bending also generates small cyclic relative displacements between the wires in contact, i.e. fretting, causing crack initiation.

Fretting on its own would not lead to wire failures: the stresses generated by the contact decrease sharply in the bulk of the material, and the initiated crack could not propagate further. Fatigue on its own could induce wire failure, but after a large number of cycles. The combination of fretting and fatigue, i.e fretting-fatigue, can lead to wire failure much faster, as fretting is responsible for crack initiation [5], and fatigue for crack propagation. It is considered to be one of the main causes of failure in wire ropes subjected to cyclic combined loads. Several researchers have tackled the effects of fretting-fatigue on the lifetime of steel wire ropes. Siegert [12] studied the effect of bending on wire ruptures in strands. He also studied the influence of fretting and fretting-fatigue on crack nucleation and propagation. Zhang et al [14] studied the effect of the crossing angle between wires. Guo et al [3] showed an evolution from mixed to gross to partial slip during the first few thousand fretting cycles. Alternatively Said et al [9,10] developed a multiscale analysis to predict the fretting-fatigue endurance of aluminum strands for overhead conductor applications. Using a global FEM modelling, the fretting-fatigue loadings generated at a contacts between wires have been estimated. Then crossed wires fretting-fatigue experiments have been performed to establish the fretting fatigue endurance of a representative contact. A multiaxial fretting-fatigue stress analysis including a critical distance correction to take into account the stress gradient effect induced by the fretting stressing has been calibrated. Using this non-local fatigue stress

analysis, a local–global prediction of the aluminum strand assembly has been established.

To prevent corrosion, grease is injected within the rope, filling all the unoccupied spaces. While the grease is not intended at improving the contact behavior, it does modify the contact environment. In this study, the effect of grease was investigated. Grease and wires were provided by the manufacturer. Wires are in high strength high carbon steel, to be used in a spiral strand rope. They are coated with a zinc layer for corrosion protection.

Experimental testing of a full rope is long and expensive. In this study, a multi-scale approach was applied. First, global tension and bending histories from a global dynamic model were applied to a detailed model of the rope developed by Martinez and Montalvo [6]. The stresses in the wires, as well as the contact forces between them, were extracted, and a typical set of conditions was chosen. These numerical local loads were then applied to single wires, using a fretting-fatigue rig. The lifetime of the wires was investigated for two environmental conditions: greased and not greased, varying independently two parameters: the contact tangential force and the fatigue stress amplitude. Dieng et al [2] studied the effect of lubrication on the fretting-fatigue behavior of steel wires, and shown a positive effect of lubrication on the fatigue limit. Most studies on the lubrication focus on the tribological behavior, such as Shima et al's [11], which shows the influence of oil on the tangential force amplitude/displacement amplitude relationship.

2. NUMERICAL MODEL

This study focuses on a 12 layers, 371 wires mooring spiral rope with a minimum breaking load of 12 500kN. The finite element model is built with Abaqus® 2021. Each wire is individually modeled with beam elements. Details on the model, are specified in [6], boundary conditions and loadings are reminded here, and shown in Figure 1.

- Embedding of the rope at the connection with floater
- Embedding of the sheath near the connection, to simulate a stiffener
- Tension in the axe of the rope
- Cyclic bending in a plane

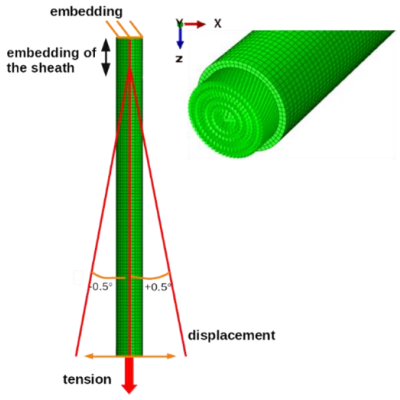

Figure 1: loadings on the numerical model

Numerical updates were done compared to [6] to lower the numerical noise, but no significative changes were implemented.

Figure 2 displays the stresses in the wires averaged over time during the cyclic bending. The layers are numbered from the inner one (layer 1) to the outer one (layer 12). Layers 1 to 3 are not shown, as the numerical noise prevents from obtaining meaningful results. Values are close to the analytical ones.

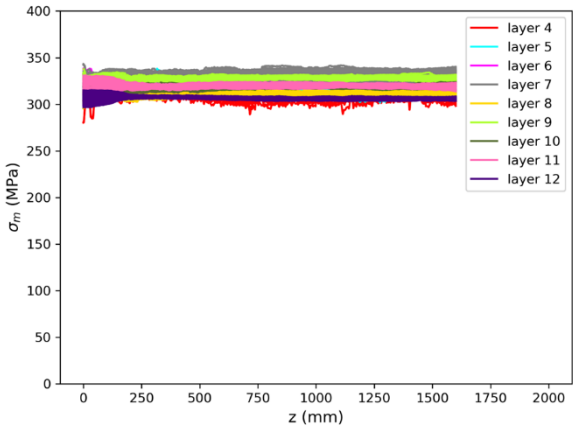

Figure 2: Mean of stresses in the wires, along the rope

Figure 3 displays the variation of stresses in the center of the wires (beam elements membrane contribution) during the cyclic bending. However, the crack initiation and propagation depends of the surface stress right under the contact. As the wires are modeled with beam elements, the stresses at the edge of the wires are not directly computed. However, using beam theory, it is possible to obtain these stresses from the axial force in the beam and the local curvature. Figure 4 displays the variation of stresses at the edge of the wires during the cyclic bending. The numerical noise is higher, and confidence in these values is lower. There is a peak at the stiffener exit, but as the stiffener is very roughly modelled, we prefer to disregard this peak.

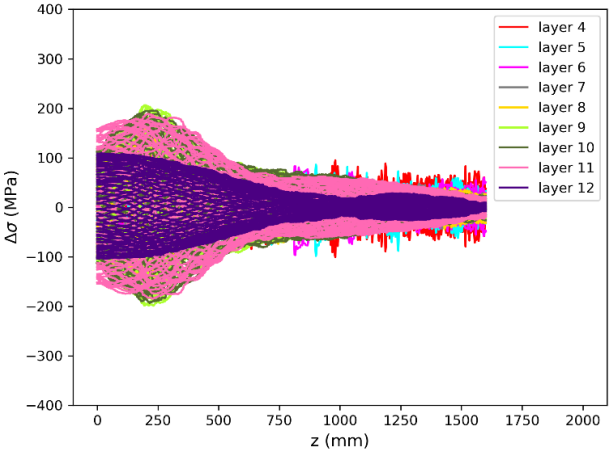

Figure 3: Variation of stresses at the center of the wires, along the rope

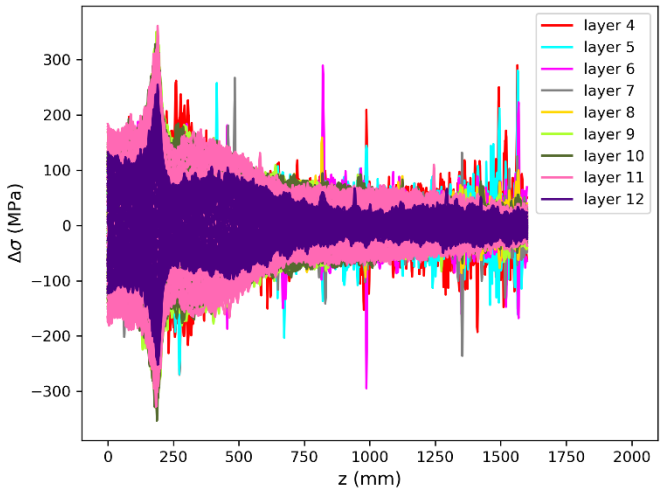

Figure 4: Variation of stresses at the edge of the wires, along the rope

The contact forces are not extracted from the simulation, as the numerical noise is too high. Instead, an analytical calculation, using a development similar to Siegert's [12], was used to calculate the normal contact forces. We note that the mean of the noisy numerical forces is coherent with the analytical results. Figure 5 displays the analytical contact forces between the wires of the different layers.

From these simulations, we extracted representative loadings for the fretting fatigue tests : stress amplitude and contact force. We took these loadings at the critical zone for fatigue, or at least where we assumed it is, since there is not yet a local fretting fatigue criterion that could spot the critical zone.

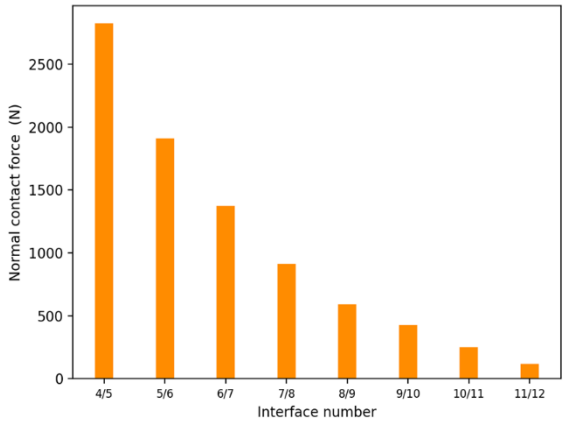

Figure 5: Analytical contact forces at the contact points between layers

3. MATERIALS AND METHODS

3.1 Materials

The tested wires are 4.85mm diameter high strength steel wires, 0.92%C and 1.2%Si, manufactured through wire drawing. Their elasticity modulus is 210 GPa, and their yield stress is 1800 MPa. They are coated with a 50μm zinc layer. Calcite grease is used for the lubricated tests.

3.2 Test rig

The testing was conducted on a two-actuators MTS hydraulic machine, similar to those used in [7,9,10]. Figure 6 displays the apparatus. The "fatigue" actuator applies a cyclic load to the specimen. A "pad wire" is in contact with the specimen with an angle $\beta = 30°$, and a normal force P is applied with a screw. To avoid specimen bending, a polymer pad is placed on the opposite side. The "fretting" actuator is connected to the pads. This second actuator allows to decouple the tangential load from the fatigue load. Load cells are used to measure both the fatigue force $F_B(t)$ and the tangential force: $Q_{total}(t) = F_B(t) - F_A(t)$. The displacement of the "fretting" actuator $\delta(t)$ is not exactly equal to the displacement of the wire pad, due to the apparatus finite stiffness, but it correlates closely. In the following, if X a cyclic signal, X^* stands for « amplitude of $X(t)$ ». The measured tangential force Q_{total} is the sum of the force applied by the polymer pad Q_{pp} and the force applied by the wire pad Q. As it is the latter that drives crack initiation, we want to use Q instead of Q_{total}. The friction coefficient between the specimen and the polymer pad $\mu_{pp} = 0.05$ was identified with tests with two polymer pads. When the polymer pad is in gross slip regime (which is the case for all our tests, as μ_{pp} is very low), Q can be calculated as $Q = Q_{total} - Q_{pp} = Q_{total} - \mu_{pp} \times P$. The material and shape of the polymer pad were chosen to minimise the friction coefficient.

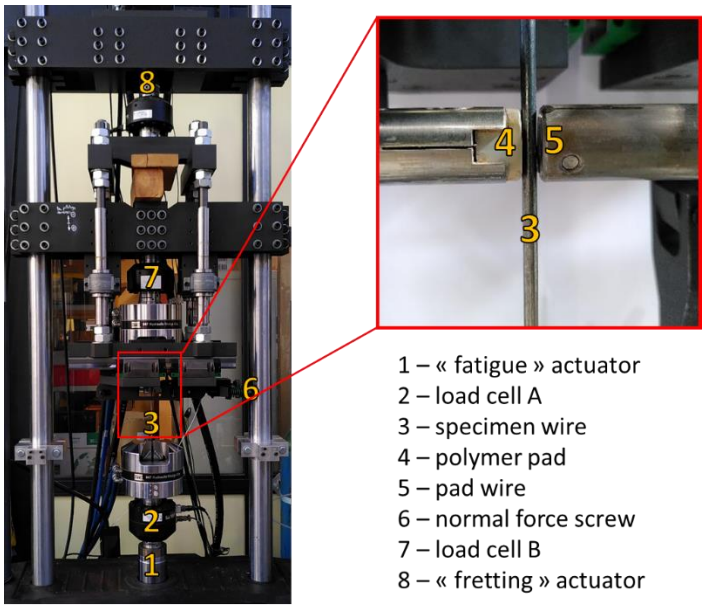

Figure 6: Fretting-fatigue experimental apparatus

The actuators are moving at the same frequency, and in the same direction. Consequently, the stress amplitude on the upper part of the specimen is higher than on the lower part, and thecracks appear preferentially on the upper bound of the fretting scar. The force F_B measured on load cell B is thus the

relevant one to predict crack initiation and propagation. The fatigue load σ is thus: $\sigma = F_B / S$, with S the specimen section. The setpoint of the fatigue actuator is adapted so that F_B^* stays constant even with changing Q_{total}^*.

When a fatigue load is applied, fretting actuator displacement δ is different from the relative displacement between the wires. An "effective displacement amplitude" is defined as $\delta_{eff}^* = \delta^* - \delta_0^*$, where δ_0^* is the displacement amplitude of the specimen at the contacting point. It can be detected experimentally: when $\delta^* = \delta_0^*$, the tangential force is null.

3.3 Fretting-fatigue tests procedure

We conducted four series of fretting-fatigue tests. In all of them, the normal force was kept constant at $P = 1400N$, as well as frequency (10Hz). In the first series, we tested clean wires, the fatigue load was kept at its "reference" values. The specimens were cleaned using a cloth soaked in ethanol. We varied fretting actuator displacement amplitudes, covering both partial slip and gross slip regimes. This was done to isolate the effect of the fretting loading, keeping the fatigue load constant. In a second series, the same sollicitations were applied to greased wires. The specimen were first cleaned using ethanol. Then the grease was heated at 60°C before application to fluidify it, as per the manufacturer instructions, and was applied on both the specimen wire and the pad wire before contact. All the tests were stopped after 1 million cycles if the specimen did not rupture before. In the third and fourth series, the fretting load was kept constant in partial slip close to the partial to gross slip transition. The first two series showed that this was the most detrimental sliding. We varied the fatigue loading. This was done to isolate the effect of the fatigue loading. The third series was conducted on clean wires, and the fourth on greased wires. The tests were stopped after 3 or 5 million cycles if the specimen did not rupture before.

4. RESULTS AND DISCUSSION

4.1 Fretting load variation, clean wires

For clean wires, once the displacement amplitude has been set, in the first few hundred cycles, the contact is always in gross slip with very low friction coefficient, but it quickly stabilize into partial slip or stable gross slip. This phenomenon was documented by Guo et al [2]. However, this has no influence on the mean of the whole duration of the test. In the figures, it is the mean over the whole duration of the test that is taken.

Figure 7 displays the lifetime of the wires in function of the displacement amplitude, and Figure 8 the corresponding normalized tangential forces amplitudes. A vertical line represents the partial to gross slip transition. In the partial slip domain, there is a linear relationship between tangential force amplitude and displacement amplitude. In the gross slip domain, the tangential force amplitude is constant: the friction coefficient is $\mu_{clean} = 0.9$. This behaviour is coherent with non-lubricated wires. Note that it is quite simple to differentiate between partial and gross slip regime thanks to the shape of the fretting cycle. Figure 9 displays the fretting cycles after 100 000 cycles for the two tests closest to the transition. The shapes indicate clearly a partial slip regime on the left, and a gross slip regime on the right. Figure 7 shows that for very small displacement amplitudes, the lifetime is over 1 million cycles. This is expected : as the tangential force is very small, cracks cannot initiate, and only the fatigue causes damage. When displacement amplitude increases, so does the tangential force, and lifetime drops to about 100 000 cycles. This is supposedly the crack initiation threshold. Lifetime is similar in the whole partial slip domain. We could have expected lifetime to drop further with increasing tangential force, as higher force could induce faster crack initiation. It seems that once the crack is initiated, its propagation is independent of the contact force. In the gross slip domain, the lifetime is over 1 million cycles. We attribute this to wear : by increasing the contact area, wear reduces the stress concentrations lower than the crack initation threshold. The threshold is very sharp : once in the gross slip domain, there is no ruptures. This contrasts with the litterature data gathered by Vingsbo and Söderberg [13] for fretting-fatigue in general : usually, there are also ruptures in the gross slip domain close to the transition, and the lifetime increases progressively when the displacement amplitude in gross slip increase. The beneficial effect of wear regarding the fretting-fatigue endurance under gross slip condition was recently formalised by Arnaud et al [1] through a combined experimental - FEM simulation of a 35NiCrMo16 steel cylinder/plan contact taking into account the surface wear, the crack nucleation and the crack propagation but also third body effects.

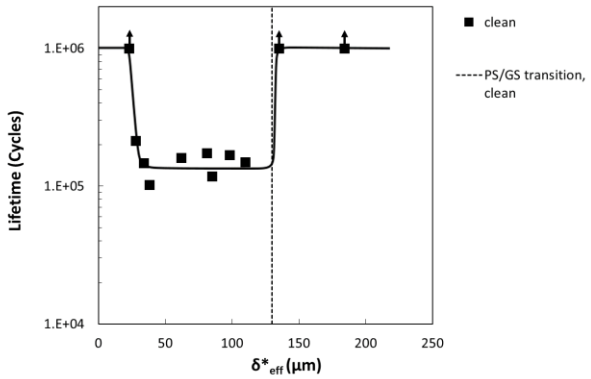

Figure 7: Lifetime in function of displacement amplitude, clean wires

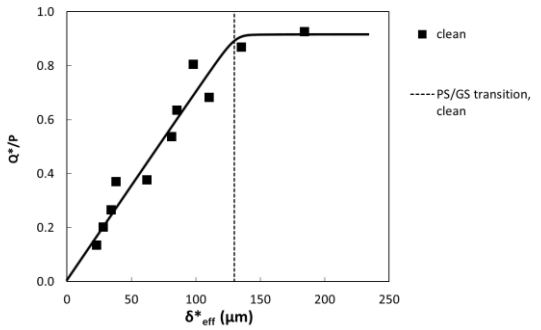

Figure 8: Normalized tangential force amplitude in function of displacement amplitude, clean wires

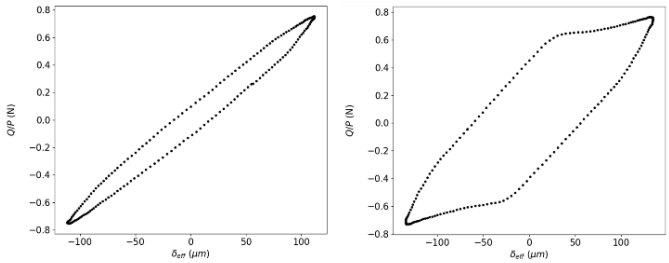

Figure 9: fretting cycles ($\delta^*_{eff} = 110\mu m$ on the left : partial slip, $\delta^*_{eff} = 125\mu m$ on the right : gross slip), clean wires

Figure 10 shows the profile of a ruptured clean wire specimen with $\delta^*_{eff} = 110\mu m$, using SEM. One can clearly see the crack initiation site, which is located right under the contact point. In the fatigue propagation zone, the crack propagates perpendicular to the wire axis. When the section becomes too small for the load, the wire breaks suddenly: this can be seen in the rupture zone. This behavior is well known : see Perier et al [8] for example.

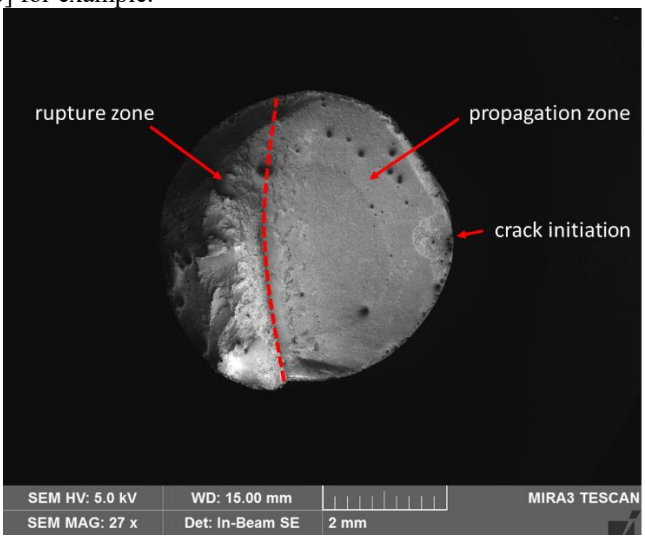

Figure 10: fracture profile (clean wire, $\delta^*_{eff} = 110\mu m$)

Figure 11 shows the fretting scar on the same specimen. The crack initiation is located at the border of the contact zone, as expected for a specimen under partial slip.

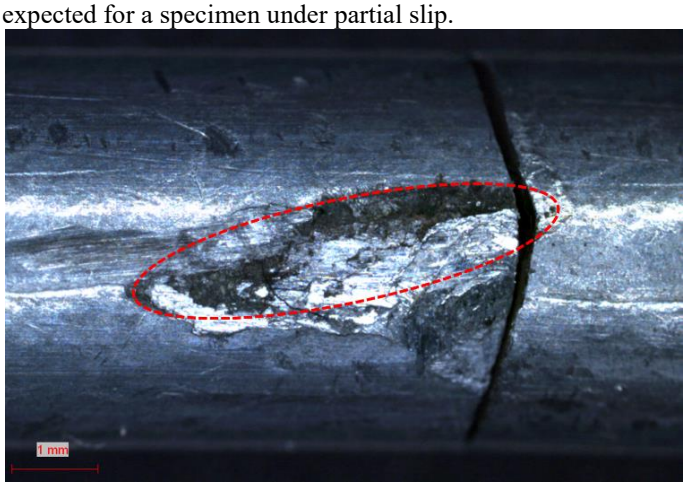

Figure 11: fretting scar (clean wire, $\delta^*_{eff} = 110\mu m$)

4.2 Fretting load variation, greased wires

For greased wires, the gross slip stabilization phase is longer than for clean wires. Its duration depends on the displacement amplitude (it is almost null for small displacement amplitudes), but is quite random, and can last from 10 000 to 100 000 cycles. This stabilization phase, in gross slip regime, produces very little fretting fatigue damage. It can be neglected for clean wires, but not for greased wires. In the following figures, we have chosen to display the lifetime corrected of this stabilization phase, as well as the mean of the tangential force starting once the stabilization phase ended.

Figure 12 displays the normalized tangential force amplitude in function of displacement amplitude for both clean and greased wires. In the gross slip domain, the friction coefficient is much lower with greased wires. In the partial slip domain, the tangential force is the same as with clean wires. It seems that the greased cannot penetrate or stay under the contact until the contact is in gross slip. This is the expected behavior for grease, as shown by Shima et al [11] and Haviez et al [4].

Figure 13 displays the lifetime of both clean and greased wires in function of imposed displacement amplitude. In gross slip regime, lifetime is over 1 million cycles. We attribute this not to wear, but to the lower friction coefficient. For $100\mu m < \delta^*_{eff} < 150\mu m$, lifetimes are the same for clean and greased wires, which seems coherent, as the tangential forces are the same. However, the crack initiation threshold is higher with greased wires ($75\mu m$) than with clean wires $25\mu m$. This is unexpected, as the fretting loads are the same. Several hypotheses can be made to explain this : an effect of the grease on the contact surface, or an effect on the crack initiation physico-chemical penomenon. Work is in progress to validate or invalidate these hypotheses.

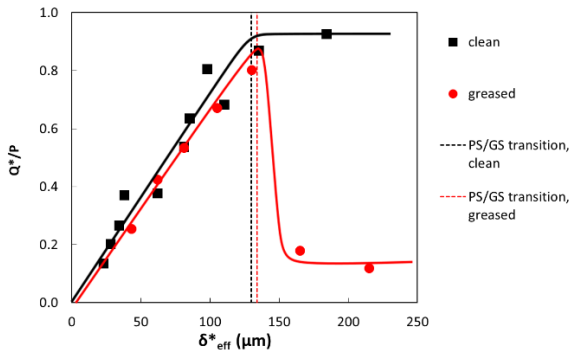

Figure 12: Normalized tangential force amplitude in function of displacement amplitude, clean and greased wires

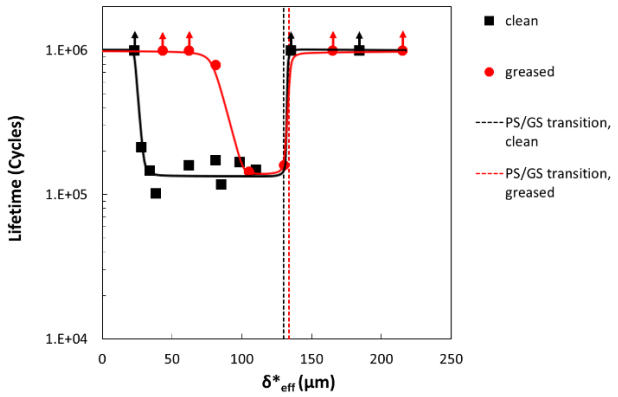

Figure 13: Lifetime in function of displacement amplitude, clean and greased wires

Hence, we observe the beneficial effect of grease lubrication on the specimens lifetime. However this beneficial effect is not constant but depends on the sliding condition. It is significant under low and medium partial slip displacement conditions but tends to zero at the partial to gross slip transition. Under gross slip condition, when surface wear is activated, both clean and lubricated conditions leads to similar fretting fatigue endurance responses. Indeed, the larger surface wear generated under clean (i.e. dry) contact promotes a sharp reduction of the contact pressure which indirectly compensates the reduction of coefficient of coefficient observed for the greased interfaces. Hence, both surface wear for clean (dry) contacts and reduction of the coefficient of friction for lubricated interfaces drastically reduce the cyclic surface shear, which in turn sharply increases the lifetime, as illustrated in Figure 13.

4.3 Fatigue load variations, clean and greased wires

Figure 14 displays the lifetime of the wires with varying fatigue amplitude, and constant tangential force ($\frac{Q^*}{P} = 0.8$). The tangential force value was chosen as close as possible to the sliding transition ($\delta^*_{eff} \sim \pm 125\mu m$) to generate the most critical fretting stresses, thus providing a conservative estimation of the fretting-fatigue endurance. The fatigue load was normalized by an arbitrary value for confidentiality reasons. The figure shows an improvement in lifetime for σ^*_a/σ_{ref} close to 1.5, but similar values for higher and lower fatigue loads. Most importantly, the fatigue limits of clean and greased wires seem to be equal. This tendency is consistent with the results displayed in Figure 13 suggesting that next to the sliding transition the grease effect is nearly negligible. The fact that longer endurances are observed in the intermediate endurance domain (i.e. medium fatigue stress range) is still an open question.

Dieng et al [2], using a mono-actuator test machine, have shown a positive effect of lubrication on the fretting-fatigue limit, which suggests that their experiments were performed under intermediate partial slip displacement conditions corresponding for our experimental configuration to displacements amplitudes between ±30 µm and ±100 µm. One advantage of the given double actuator fretting test machine (compared to any mono-actuator experiment) is the possibility to monitor the fretting contact displacement and therefore to separate the effects of fretting (i.e. contact) and fatigue loadings. If lower fretting loadings had been chosen ($i.e.\ \delta^*_{eff} < 100\mu m$), we expected longer fretting fatigue endurance for the greased interface than the clean, as suggested by Figure 13 and Dieng et al's results.

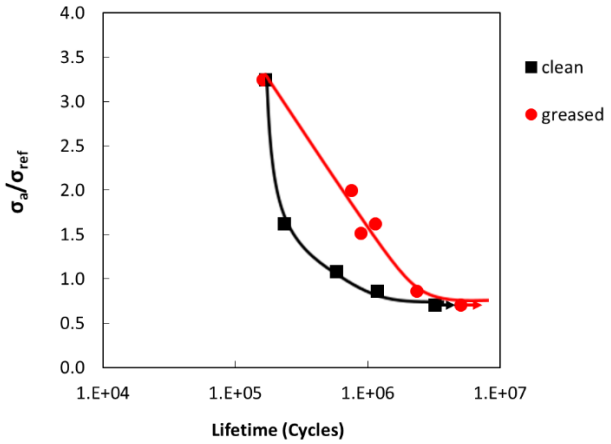

Figure 14: Lifetime in function of fatigue amplitude, clean and greased wires

5. CONCLUSION

In this paper, the effect of grease on fretting-fatigue lifetime was investigated. A two actuator rig allowed for complete decoupling of fretting and fatigue sollicitations. Results show that the fatigue limit, when keeping the fretting load constant, is not affected by the presence of grease. They also show an unexplained positive effect of grease in the partial slip domain. Further investigations are needed to understand this effect, and if it is possible to expand it to the whole partial slip domain. This work provides opportunities for selecting,

testing or developing greases with better lubrication power, that will improve the fatigue life of steel ropes in tension and bending.

ACKNOWLEDGEMENTS

The authors would like to thank ArcelorMittal Bourg-en-Bresse for providing the test specimens and for the useful advices.

REFERENCES

[1] P. Arnaud and S. Fouvry. 2020. Modeling the fretting fatigue endurance from partial to gross slip: The effect of debris layer. *Tribology International* 143, (March 2020), 106069. DOI:https://doi.org/10.1016/j.triboint.2019.106069

[2] Lamine Dieng, J.R. Urvoy, D. Siegert, P Brevet, Virginie Perier, and C. Tessier. Assessment of lubrication and zinc coating on the high cycle fretting fatigue behaviour of high strength steel wires. *OIPEEC Conference Proceedings*, 85,97.

[3] Tong Guo, Zhongxiang Liu, José Correia, and Abílio M.P. de Jesus. 2020. Experimental study on fretting-fatigue of bridge cable wires. *International Journal of Fatigue* 131, (February 2020), 105321. DOI:https://doi.org/10.1016/j.ijfatigue.2019.105321

[4] L. Haviez, S. Fouvry, and G. Yantio. 2016. Investigation of grease behavior under simple and complex displacement amplitudes conditions. *Tribology International* 100, (August 2016), 186–194. DOI:https://doi.org/10.1016/j.triboint.2016.01.017

[5] R. E. Hobbs and M. Raoof. 1994. Mechanism of fretting fatigue in steel cables. *International Journal of Fatigue* 16, 4 (June 1994), 273–280. DOI:https://doi.org/10.1016/0142-1123(94)90341-7

[6] Michaël Martinez and Sébastien Montalvo. 2020. Detailed Finite Element Modeling of a High Capacity Mooring Steel Wire Rope: Calculation of the Stress Concentration Near the Connection. American Society of Mechanical Engineers Digital Collection. DOI:https://doi.org/10.1115/OMAE2020-18170

[7] J. Meriaux, S. Fouvry, K. J. Kubiak, and S. Deyber. 2010. Characterization of crack nucleation in TA6V under fretting–fatigue loading using the potential drop technique. *International Journal of Fatigue* 32, 10 (October 2010), 1658–1668. DOI:https://doi.org/10.1016/j.ijfatigue.2010.03.008

[8] V. Périer, L. Dieng, L. Gaillet, C. Tessier, and S. Fouvry. 2009. Fretting-fatigue behaviour of bridge engineering cables in a solution of sodium chloride. *Wear* 267, 1–4 (June 2009), 308–314. DOI:https://doi.org/10.1016/j.wear.2008.12.107

[9] J. Said, S. Garcin, S. Fouvry, G. Cailletaud, C. Yang, and F. Hafid. 2020. A multi-scale strategy to predict fretting-fatigue endurance of overhead conductors. *Tribology International* 143, (March 2020), 106053. DOI:https://doi.org/10.1016/j.triboint.2019.106053

[10] Julien Said, Siegfried Fouvry, Georges Cailletaud, Christine Yang, and Fikri Hafid. 2020. Shear driven crack arrest investigation under compressive state: Prediction of fretting fatigue failure of aluminium strands. *International Journal of Fatigue* 136, (July 2020), 105589. DOI:https://doi.org/10.1016/j.ijfatigue.2020.105589

[11] M. Shima, H. Suetake, I. R. McColl, R. B. Waterhouse, and M. Takeuchi. 1997. On the behaviour of an oil lubricated fretting contact. *Wear* 210, 1 (September 1997), 304–310. DOI:https://doi.org/10.1016/S0043-1648(97)00078-1

[12] D. Siegert. 1997. Mecanismes de fatigue de contact dans les cables de haubanage du genie civil.

[13] Olof Vingsbo and Staffan Söderberg. 1988. On fretting maps. *Wear* 126, 2 (September 1988), 131–147. DOI:https://doi.org/10.1016/0043-1648(88)90134-2

[14] Dekun Zhang, Xuehui Yang, Kai Chen, and Zefeng Zhang. 2018. Fretting fatigue behavior of steel wires contact interface under different crossing angles. *Wear* 400–401, (April 2018), 52–61. DOI:https://doi.org/10.1016/j.wear.2017.12.014